Journal of Cerebral Blood Flow & Metabolism (2012) 32, 150–163

www.jcbfm.com

Fibrinogen-induced increased pial venular permeability in mice

Nino Muradashvili[1], Natia Qipshidze[1], Charu Munjal[1], Srikanth Givvimani[1], Richard L Benton[2], Andrew M Roberts[1], Suresh C Tyagi[1] and David Lominadze[1]

[1]*Department of Physiology and Biophysics, University of Louisville, School of Medicine, Louisville, Kentucky, USA;* [2]*Department of Neurological Surgery and Kentucky Spinal Cord Injury Research Center, University of Louisville, School of Medicine, Louisville, Kentucky, USA*

Elevated blood level of Fibrinogen (Fg) is commonly associated with vascular dysfunction. We tested the hypothesis that at pathologically high levels, Fg increases cerebrovascular permeability by activating matrix metalloproteinases (MMPs). Fibrinogen (4 mg/mL blood concentration) or equal volume of phosphate-buffered saline (PBS) was infused into male wild-type (WT; C57BL/6J) or MMP-9 gene knockout (MMP9−/−) mice. Pial venular leakage of fluorescein isothiocyanate-bovine serum albumin to Fg or PBS alone and to topically applied histamine (10^{-5} mol/L) were assessed. Intravital fluorescence microscopy and image analysis were used to assess cerebrovascular protein leakage. Pial venular macromolecular leakage increased more after Fg infusion than after infusion of PBS in both (WT and MMP9−/−) mice but was more pronounced in WT compared with MMP9−/− mice. Expression of vascular endothelial cadherin (VE-cadherin) was less and plasmalemmal vesicle-associated protein-1 (PV-1) was greater in Fg-infused than in PBS-infused both mice groups. However, in MMP9−/− mice, VE-cadherin expression was greater and PV-1 expression was less than in WT mice. These data indicate that at higher levels, Fg compromises microvascular integrity through activation of MMP-9 and downregulation of VE-cadherin and upregulation of PV-1. Our results suggest that elevated blood level of Fg could have a significant role in cerebrovascular dysfunction and remodeling.
Journal of Cerebral Blood Flow & Metabolism (2012) **32,** 150–163; doi:10.1038/jcbfm.2011.144; published online 12 October 2011

Keywords: cerebrovascular permeability; endothelial cell cadherin; intercellular adhesion molecule-1; macromolecular leakage; matrix metalloproteinases

Introduction

Fibrinogen (Fg) is a high molecular weight plasma adhesion glycoprotein that is primarily synthesized in hepatocytes. Inflammatory cytokines interleukin-1 and interleukin-6 are involved in Fg synthesis. During inflammation, overexpression of interleukin-1 and interleukin-6 leads to an increased blood content of Fg (Nakamura *et al*, 1996). Elevated blood level of Fg is a biomarker of inflammation and high risk factor for many cardiovascular (Danesh *et al*, 2005) and cerebrovascular disorders (del Zoppo *et al*, 2009) such as hypertension (Lominadze *et al*, 1998) and stroke (Eidelman and Hennekens, 2003). While normal blood concentration of Fg is about 2 mg/mL (Lominadze *et al*, 2010), during hypertension it reaches 4 mg/mL (Lominadze *et al*, 1998) and 3.6 mg/mL after ischemic stroke in humans (Eidelman and Hennekens, 2003).

Vasoactive effects of isolated peptides derived from plasmin digestion of fibrin and Fg were studied in various vascular beds; however, results are controversial. Infusion of fragment D into conscious rabbits increased vascular permeability to albumin (Manwaring and Curreri, 1981), while in another study, infusion of fragment D in sheep did not alter pulmonary transvascular fluid and protein exchange (Johnson *et al*, 1985).

The vasoactive property of undegraded Fg was first shown by Hicks *et al* (1996). We showed that high content of undegraded Fg can cause an arteriolar constriction (Lominadze *et al*, 2005) and disruption of endothelial cell (EC) layer integrity (Patibandla *et al*, 2009; Tyagi *et al*, 2008).

It is well documented that digestion of Fg by plasmin *in vivo* is quite rare (Gaffney, 2001). During

Correspondence: Dr D Lominadze, Associate Professor, Department of Physiology and Biophysics, University of Louisville, School of Medicine, Building A, Room 1115, 500 South Preston Street, Louisville, KY 40202, USA.
E-mail: david.lominadze@louisville.edu
This study was supported in part by NIH Grants HL-80394, HL-80394S2 (to DL), HL-71010, and NS-051568 (to SCT).
Received 10 July 2011; revised 17 August 2011; accepted 12 September 2011; published online 12 October 2011

many inflammatory diseases (e.g., hypertension), increased content of Fg and plasminogen-activator inhibitor type 1 leads to a decreased fibrinolysis and accumulation of Fg (Landin *et al*, 1990). Thus, higher content of undegraded Fg may contribute to the development of inflammatory responses.

One of the indications of inflammation is a microvascular leakage of plasma substances and proteins and their deposition in SEM (subendothelial matrix) and interstitium (Mehta and Malik, 2006). These alterations exacerbate complications of blood circulation during vascular diseases and cause edema (Lominadze *et al*, 2010; Mehta and Malik, 2006). Blood plasma components may pass through the endothelial barrier via two paracellular and transcellular transport mechanisms (Mehta and Malik, 2006; Simionescu *et al*, 2009). Movement of substances via the paracellular pathway occurs between the ECs and involves alterations in tight, gap, and adherence junction proteins (Mehta and Malik, 2006). Vascular endothelial cadherin (VE-cadherin), which is a strictly endothelial-specific adhesion molecule, is located at the basal side of the ECs (Mehta and Malik, 2006; Vestweber, 2008). Its presence at cell contacts is an essential step that indicates the extent of permeability of blood vessels through the paracellular pathway (Vestweber, 2008). The transcellular transport is implemented by movement of substances across an EC layer by caveolae, caveolae generated transendothelial channels, and fenestrae (Simionescu *et al*, 2009). Plasmalemmal vesicle-associated protein-1 (PV-1) is an integral membrane-associated protein of caveolae found in fenestral and stomatal diaphragms in fenestrated endothelial and transendothelial channels (Hnasko *et al*, 2002). It is considered a functional biomarker for altered vascular permeability following central nervous system trauma (Mozer *et al*, 2010) and disruption of blood–brain barrier (BBB) (Shue *et al*, 2008). Thus, the combination and the functional balance of these two pathways govern the net transport of substances in microcirculation.

Matrix metalloproteinases (MMPs) are zinc-dependent endoproteinases expressed in various cell types including ECs. They are involved in both physiological and pathological processes, especially in SEM degradation and vascular remodeling that disrupt the BBB (Rosell *et al*, 2006). Activation of MMP-9, the most abundant MMP, has an important role in decreasing of brain vascular endothelial layer integrity through degradation of EC junction proteins and causing macromolecular leakage (Rosell *et al*, 2006).

Since pial arterioles are resistance vessels that control global blood supply to the brain (Cohen *et al*, 1996), it is important to investigate the role of increased blood content of Fg in pial circulation. Increased venular leakage leads to edema formation in the microcirculatory bed affecting the arteriolar function. Therefore, in the present study, we tested the hypothesis that increased content of Fg can cause a macromolecular leakage in mouse pial venules. Our findings show that an elevated blood level of undegraded Fg has a considerable role in the development of cerebrovascular macromolecular leakage, and the process can be mitigated by inhibition of MMP-9 activity, suggesting that changes in the blood level of Fg may have a significant role in microvascular remodeling during inflammatory cerebrovascular diseases.

Materials and methods

Animals

In accordance with the National Institute of Health Guidelines for animal research, all animal procedures for these experiments were reviewed and approved by the Institutional Animal Care and Use Committee of the University of Louisville.

Male wild-type (WT) C57BL/6J and MMP-9 gene knockout (MMP9−/−) homozygous (FVB.Cg-*Mmp9*^{tm1Tvu}/J; stock number: 004104) and its control FVB (FVB/NJ; stock number: 001800) mice were obtained from the Jackson Laboratory (Bar Harbor, ME, USA). For genotyping of MMP9−/− mice, DNA was extracted from the tail tip of mice and was amplified by polymerase chain reaction using specific primer sequences according to the protocol provided by the Jackson Laboratory. The primer sequences for MMP9−/− were forward: 5′-CTGAATGAACTGCAGGA CGA-3′; reverse: 5′-ATACTTTCTCGGCAGGAGCA-3′. The primer sequences for WT were forward: 5′-GTGGGACCATC ATAACATCACA-3′; reverse: 5′-CTCGCGGCAAGTCTTCAG AGTA-3′.

Twelve-week old mice (26 to 30 g) were anesthetized with sodium pentobarbital (70 mg/kg, intraperitoneally). Supplemental anesthesia was given as required during the experiment. In all, 2% Xylocaine (AstraZeneca LP, Wilmington, DE, USA) was used for local analgesia. The left carotid artery was cannulated with polyethylene tubing PE-10 for blood pressure monitoring and necessary infusions. The trachea was cannulated to maintain a patent airway. Body temperature was kept at 37°C ± 1°C with a heating pad. Mean arterial blood pressure and heart rate were continuously monitored through a carotid artery cannula connected to a transducer and a blood pressure analyzer (CyQ 103/302, Cybersense, Lexington, KY, USA) and by a tail cuff and a CODA monitor, a noninvasive blood pressure measurement system (Kent Scientific Apparatus, Torrington, CT, USA). The mean arterial blood pressure monitoring with the tail cuff was necessary to detect possible blood pressure changes during infusion of phosphate-buffered saline (PBS), Fg, or Dextran-410.

Reagents and Antibodies

Human Fg (FIB-3, depleted of plasminogen, von-Willebrand factor, and fibronectin) was purchased from Enzyme Research Laboratories (South Bend, IN, USA). Purified antibody against mouse intracellular adhesion molecule-1 (ICAM-1; CD54—clone: YN1/1.7.4; Isotype: Rat IgG2b,κ) was obtained from BioLegend (San Diego, CA,

USA). Anti-mouse VE-cadherin (goat polyclonal IgG, Cdh5 (mouse), clone: C-19) and 4,6-diamidino-2-phenyl-indole HCl (DAPI) were from Santa Cruz Biotechnology (Santa Cruz, CA, USA). Rat anti-mouse PV-1 monoclonal antibody (clone: MECA-32; Isotype: IgG2a) was from AbD Serotec (Raleigh, NC, USA). DQ-gelatin, 1,10-phenanthroline, monohydrate, and secondary antibodies conjugated with Alexa-fluor 488 (chicken anti-rat IgG), or with Alexa-fluor 594 (chicken anti-rat IgG and rabbit anti-goat IgG) were purchased from Invitrogen (Carlsbad, CA, USA). Bovine serum albumin (BSA) and Dextran-410 were from Sigma-Aldrich Chemicals Co. (St Louis, MO, USA). Normal Donkey Serum was obtained from Jackson Immuno Research (West Grove, PA, USA). Tetramethylrhodamine β-isothiocyanate (TRITC)- or fluorescein isothiocyanate (FITC)-conjugated *Lycopersicon esculentum* agglutinin (LEA) tomato lectin was from Vector Laboratories (Burlingame, CA, USA). Artificial cerebrospinal fluid (composition: *Na* 150 mmol/L *Na*; 3.0 mmol/L *K*; 1.4 mmol/L *Ca*; 0.8 mmol/L *Mg*; 1.0 mmol/L *P*; 155 mmol/L *Cl*) was purchased from Harvard Apparatus (Holliston, MA, USA).

Cranial Window Preparation

The brain pial microcirculation was prepared for observations as previously described (Lominadze *et al*, 2006), Briefly, a mouse was placed on a stereotaxic apparatus (World Precision Instruments, Sarasota, FL, USA). The scalp and connective tissues were removed over the parietal cranial bone above the left hemisphere. A craniotomy was done with a small (1.8 mm in diameter) trephine attached to a high-speed microdrill (Fine Science Tools, Foster City, CA, USA). During drilling, the cranium was continuously irrigated with room temperature PBS. The dura matter was lifted with the bone disk using a microrongeur with extra-fine tips (Fine Science Tools) to form a cranial window. The surface of the exposed pial circulation was continuously superfused with cerebrospinal fluid. Constant temperature (37°C) of cerebrospinal fluid was maintained by dual automatic temperature controller (Warner Instrument Corporation, Hamden, CT, USA). It has been found that responses of pial vessels observed from an opened cranial window are representative of the responses of the pial microcirculation (Rosenblum and El-Sabban, 1982).

Microvascular Leakage Observation

Fibrinogen-induced pial vascular leakage was observed according to the method described previously (Lominadze *et al*, 2006). Mice were positioned on the stage of an Olympus BXG61WI microscope (Olympus, Tokyo, Japan) so that the exposed pial circulation could be observed by epi-illumination. Following the surgical preparation and preceding each experiment, there was a 1-hour equilibration period. Before each experiment, autofluorescence of the observed area was recorded over a standard range of camera gains. Fluorescein isothiocyanate (300 μg/mL) bound to BSA (FITC-BSA) was infused through the carotid artery cannulation. Before infusion, to remove possibly formed free FITC, FITC-BSA solution was dialyzed against PBS solution using a dialyzing cassette with cutoff size of 15 kDa (Thermo Scientific, Rockford, IL, USA). Fluorescein isothiocyanate-BSA was infused (0.2 mL/100 g of body wt.) for over 10 minutes time period by a syringe pump (Harvard Apparatus) and allowed to circulate for about 10 minutes (Lominadze *et al*, 2006). The pial circulation was surveyed to ensure that there was no spontaneous leakage in the observed area that would indicate decreased vascular integrity. Venules were identified by observing the topology of the pial circulation and blood flow direction (vascular diameters increasing in the direction of blood flow). Images of the selected third-order venular segments were recorded and used as baseline.

Fibrinogen (20 mg per 100 g of body weight) was infused (20 μL/min, over 10 minutes time period) through the carotid artery cannulation into the experimental mice. This dose of Fg resulted in a total blood content of Fg of about 4 mg/mL. Mice in the control group were infused with the same volume of PBS as they would have been infused with Fg. Ten minutes after completion of infusion, images of the selected venular segments were recorded. Then, histamine doses (10^{-6}, 10^{-5}, and 10^{-4} mol/L in 50 μL of cerebrospinal fluid) were applied topically with 10-minute intervals between doses. In preliminary experiments, we found that 10^{-6} mol/L histamine did not have an effect and that 10^{-4} mol/L histamine induced extensive macromolecular leakage of pial venules. Therefore, we chose to focus on 10^{-5} mol/L histamine for the remainder of the studies.

An epi-illumination system, consisting of a mercury arc lamp and a ploem system with appropriate filters, was used to observe intravascular FITC. The area of interest (AOI) was exposed to blue light (488 nm) for 10 to 15 seconds with a power density of 3.5 μW/cm^2. The microscope images were acquired by an electron-multiplying charge-coupled device camera (Quantem 512SC; Photometrics, Tucson, AZ, USA) and image acquisition system (Slidebook 5.0, Intelligent Imaging Innovations, Inc., Philadelphia, PA, USA). The camera output was standardized with a 50-ng/mL fluorescein diacetate standard (Estman Kodak, Rochester, NY, USA) for each experiment. The lamp power and camera gain settings were held constant during the experiments, and the camera response was verified to be linear over the range used for these acquisitions. The magnification of the system with Olympus $\times$10/0.40 (UPlanSApo) objective was determined with a stage micrometer and vessel diameters were measured with the Slidebook 5.0.

Images of the pial venular circulation were analyzed by image analysis software (Image-Pro Plus 6.3, Media Cybernetics, Bethesda, MD, USA). In each image, a rectangular AOI of about 1,300 μm^2 was positioned in the interstitium adjacent to a venular wall to assess macromolecular leakage to the interstitium. The AOI was positioned in the interstitial region with no spontaneous leakage (defined by comparison to the background) or a visible microvessel. Another AOI (700 μm^2) was positioned in the middle of a target venule. Fluorescence intensity values measured after infusion of Fg or PBS are presented as percent of baseline values recorded 10 minutes before Fg

or PBS infusion, respectively. Histamine-induced changes in fluorescence intensity in the AOI were measured 10 minutes after its topical application and are presented as percent of baseline recorded before histamine application.

At the end of the experiments, blood was collected to obtain plasma samples (Lominadze *et al*, 1998) and an extent of Fg degradation was assessed. The purity of plasma Fg was compared with infused Fg by Coomassie-stained sodium dodecyl sulfate polyacrylamide gel electrophoresis gel (8%) analysis under reducing conditions.

To validate that infusion of FITC-BSA alone does not cause microvascular leakage, pial venules were observed for 60 minutes, with no additional infusion of PBS or Fg. In another series of experiments, Dextran-410 was infused at the same concentration as Fg to define a possible role of Fg-induced blood viscosity changes on vascular permeability. Pial venular leakage of FITC-BSA was observed as described above. Similarity in the viscosity of 4 mg/mL Fg and 4 mg/mL of Dextran-410 was validated with a 'cone and plate' type viscometer (LVDV-II, Brookfield Engineering Laboratories, Inc., Stoughton, MA, USA).

Immunohistochemistry

At the completion of experiments, mice were infused with FITC- or TRITC-conjugated LEA via the carotid cannulation to fluorescently label moieties on the intravascular surface (Mozer *et al*, 2010). Animals were killed with an anesthetic overdose, infused immediately with PBS through the left ventricle for exsanguination. The cranium was opened and the brain was gently dissected and removed for fresh tissue processing. Mouse brain tissue immunohistochemistry was done according to the method described earlier (Mozer *et al*, 2010). The brain was mounted in protective matrix (Polyscience, Inc., Warrington, PA, USA) and cryosectioned using a Leica CM 1850 Cryocut (Bannockburn, IL, USA). Thirty 30-μm thick slices were thaw mounted on charged microscope slides (VWR, West Chester, PA, USA) and stored at -80°C. Before immunostaining, slides were kept at -20°C overnight, and then warmed at 37°C for 20 minutes and mounting matrix was removed. The sections were postfixed in ice-cold 100% methanol for 10 minutes, washed three times in TBS (Tris-buffered saline) and blocked for nonspecific epitope binding in 0.1% TritonX-100 TBS (TBS-T), 0.5% BSA, and 10% Normal Donkey Serum for 1 hour at room temperature.

Immunohistochemistry and laser-scanning confocal microscopy were used to detect Fg-induced changes in ICAM-1, VE-cadherin, and PV-1 expression in the brain vasculature. Fibrinogen-induced expression of ICAM-1, an endothelial receptor for Fg (Plow *et al*, 2000) was tested in the brain samples not infused with LEA. Expressions of VE-cadherin, PV-1, which is considered to be associated with caveolae and transendothelial channels in fenestrated endothelium (Hnasko *et al*, 2002), and Dextran-induced ICAM-1 were detected in samples obtained from LEA-infused mice. Primary antibodies (anti-ICAM-1, dilution 1:500; anti-VE-cadherin, dilution 1:250; or anti-PV-1, dilution 1:500) were applied to the brain slices overnight in a humidified chamber placed on a rotator at 4°C. After washing, the corresponding fluorescent dye-conjugated secondary antibodies (dilution 1:500) were applied for 1 hour at room temperature. Cell nuclei were labeled with DAPI (1:1,000). The laser-scanning confocal microscope (Olympus FluoView1000, objective $\times 100$) was used for image capture. VE-cadherin, ICAM-1, and TRITC-LEA were visualized using a HeNe-G laser (556 nm) to excite the dye, while emission was observed above 573 nm. Fluorescein isothiocyanate-LEA and PV-1 were visualized using a Multi Argon laser (495 nm) to excite the dye, while emission was observed above 519 nm. Cell nuclei (DAPI) were visualized using a 405-laser diode laser (372 nm) to excite the dye, while emission was observed above 456 nm. Since in each of these experiments we compared the fluorescence intensities between the groups, fluorescence intensity (for each color) was adjusted to its saturation point in an experimental group with the maximum fluorescence intensity for the color of interest and the laser and multipliers' settings were kept unaltered during measurements in each experimental series.

Off-line image analysis software (Image-Pro Plus) was used to assess ICAM-1, VE-cadherin, and PV-1 expression. To assess expression of ICAM-1, fluorescence intensity was measured in the AOI (of the same size in all experimental groups) placed in the inner surface of a vessel. For detection of VE-cadherin or PV-1, corresponding AOIs (of the same size in all respective experimental groups) were placed along the vessel wall. For each experimental group, three to four brain slices were analyzed. In each brain slice, three to five vascular images were analyzed for ICAM-1, VE-cadherin, or PV-1 expression and normalized per length of the respective vascular segment. Fluorescence intensity in four randomly placed AOIs were measured. The results were averaged for each experimental group and presented as fluorescence intensity units (FIU).

In Tissue Zymography

Gelatinolytic activity of MMPs was demonstrated by in tissue zymography according to a modified protocol described elsewhere (Mook *et al*, 2003). DQ-gelatin was used as a substrate while 1,10-phenanthroline,monohydrate, a general metalloproteinase inhibitor, was used as a negative control. Unfixed mouse brain cryostat sections (15-μm thick) were warmed for 20 minutes. DQ-gelatin was dissolved in water to 1 mg/mL concentration according to the manufacturer's recommendation, placed on the sections, and incubated for 2 hours on a rotator at room temperature. Samples were incubated with DAPI for 10 minutes. After washing with PBS, the slides were covered with glass coverslips. Laser-scanning confocal microscope (objective $\times 100$) was used to capture the images. Fluorescence was detected with the excitation at 484 nm and emission at 512 nm. Off-line image analysis was used to assess MMP activity. The fluorescence intensity (a measure of MMP activity) was measured in same size AOI in all the experimental groups. For each experimental group, three to four brain slices were

analyzed. In each brain slice, four to five vascular images were analyzed for MMP activity assessment. Fluorescence intensity in four randomly placed AOIs was measured and normalized per vascular segment length. The results are averaged for each experimental group and presented as FIU.

Data Analysis

All data are expressed as mean ± s.e.m. The experimental groups were compared by one-way analysis of variance. If analysis of variance indicated a significant difference ($P < 0.05$), Tukey's multiple comparison test was used to compare group means. Differences were considered significant if $P < 0.05$.

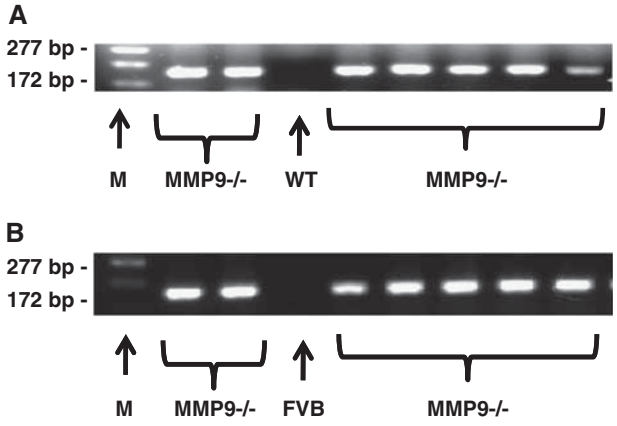

Figure 1 Genotyping of matrix metalloproteinase-9 (MMP-9) gene knockout (MMP9−/−), wild-type (WT), and FVB mice. Single polymerase chain reaction (PCR) products suggest the homozygous mutation (**A**, **B**), while its absence represents WT (**A**) or FVB (**B**) allele.

Table 1 Comparison of body weight (bd. wt.), mean arterial blood pressure (MABP), and heart rate (HR) in wild-type (WT), FVB, and MMP-9 gene knockout (MM9−/−) mice infused with phosphate-buffered saline (PBS) or fibrinogen (Fg)

	WT		*FVB*		*MMP9−/−*	
	PBS	*Fg*	*PBS*	*Fg*	*PBS*	*Fg*
Bd. wt. (g)	25 ± 3	26 ± 4	26 ± 3	26 ± 5	26 ± 4	26 ± 3
MABP (mm Hg)	113 ± 5	126 ± 6	112 ± 7	120 ± 8	115 ± 7	120 ± 8
HR (b.p.m.)	394 ± 16	403 ± 12	388 ± 12	390 ± 9	389 ± 11	390 ± 11

MMP, matrix metalloproteinase.
All values are mean ± s.e.m. $n = 8$.

Results

Macromolecular Leakage from Pial Venules

Genotyping of MMP9−/− mice using appropriate primers and polymerase chain reaction confirmed that MMP9−/− mice lack MMP-9 gene in comparison to WT and FVB mice (Figure 1). Body weight of animals used in the study was similar (Table 1). Mean arterial blood pressure and heart rate did not change after infusion of PBS or Fg in WT, FVB, and MMP9−/− mice (Table 1).

Diameters of observed pial venules did not change after infusion of PBS (48 ± 8 μm) or Fg (42 ± 5 μm) compared with their baseline values (43 ± 5 and 47 ± 4 μm, respectively; $n = 8$ in both groups) in WT mice. Similarly, pial venular diameters did not change after infusion of PBS (46 ± 6 μm) or Fg (42 ± 6 μm) compared with their baseline values (44 ± 6 and 48 ± 3 μm, respectively; $n = 8$ in both groups) in FVB mice. In MMP9−/− mice, changes in venular diameters in response to PBS (46 ± 7 μm) or Fg (44 ± 4 μm) infusion were even less compared with their baseline values (42 ± 4 and 47 ± 5 μm, respectively; $n = 8$ in both groups). Application of histamine (10^{-5} mol/L) did not change venular diameters in WT (54 ± 7 μm after PBS and 44 ± 5 μm after Fg infusion; $n = 8$ in both groups), FVB (53 ± 6 μm after PBS and 43 ± 6 μm after Fg infusion; $n = 8$ in both groups), or in MMP9−/− (48 ± 4 μm after PBS and 45 ± 5 μm after Fg infusion; $n = 8$ in both groups) mice.

In WT mice, Fg induced greater pial venular leakage compared with the group infused with PBS (Figure 2). Similarly, in MMP9−/− mice, venular leakage after Fg infusion was greater than that after PBS infusion, but less than that in respective groups of WT mice (Figure 2). After topical application of histamine (10^{-5} mol/L), venular leakage was increased in WT and MMP9−/− groups (Figure 2). However, it was greater in both mice groups infused with Fg compared with those infused with PBS and was less in MMP9−/− mice than in the respective

Figure 2 Fibrinogen (Fg)-induced macromolecular leakage of pial venules. (**A**) Examples of images recorded before (baseline; first row), after infusion of Fg (final blood concentration 4 mg/mL) or phosphate-buffered saline (Fg or PBS; second row), and topical application of histamine (10^{-5} mol/L) (third row), in wild-type (WT; first two columns), FVB (second pair of columns), and matrix metalloproteinase-9 (MMP-9) gene knockout (MMP9−/−; third pair of columns) mice. Microvascular leakage was assessed by fluorescence intensity of fluorescein isothiocyanate-bovine serum albumin (FITC-BSA) in the rectangular area of interest (AOI) shown on images. (**B**) Summary of changes in fluorescence intensity after infusion of Fg or PBS measured in the AOI. $P < 0.05$ for all. *—versus WT-PBS, #—versus WT-Fg, †—versus FVB-PBS, ‡—versus FVB-Fg, §—versus (MMP9−/−)-PBS ◆—versus (MMP9−/−)-Fg, ♣—versus WT + PBS/Hist, ¶—versus WTFg/Hist; @—versus FVB-PBS/Hist, ®—versus FVB-Fg/Hist, ©—versus MMP-PBS/Hist. $n = 8$ for all groups. Inset: Purity of Fg with no visible extra bands lighter than ~49 kDa (that would indicate degradation products) was confirmed by the Coomassie-stained sodium dodecyl sulfate polyacrylamide gel electrophoresis (SDS-PAGE) analysis.

groups of WT mice (Figure 2). In FVB mice, pial venular leakage induced by PBS infusion was not different from that in WT mice (Figure 2). Similarly, macromolecular leakage of pial venules of FVB mice induced by Fg infusion was not different from that induced in WT mice (Figure 2).

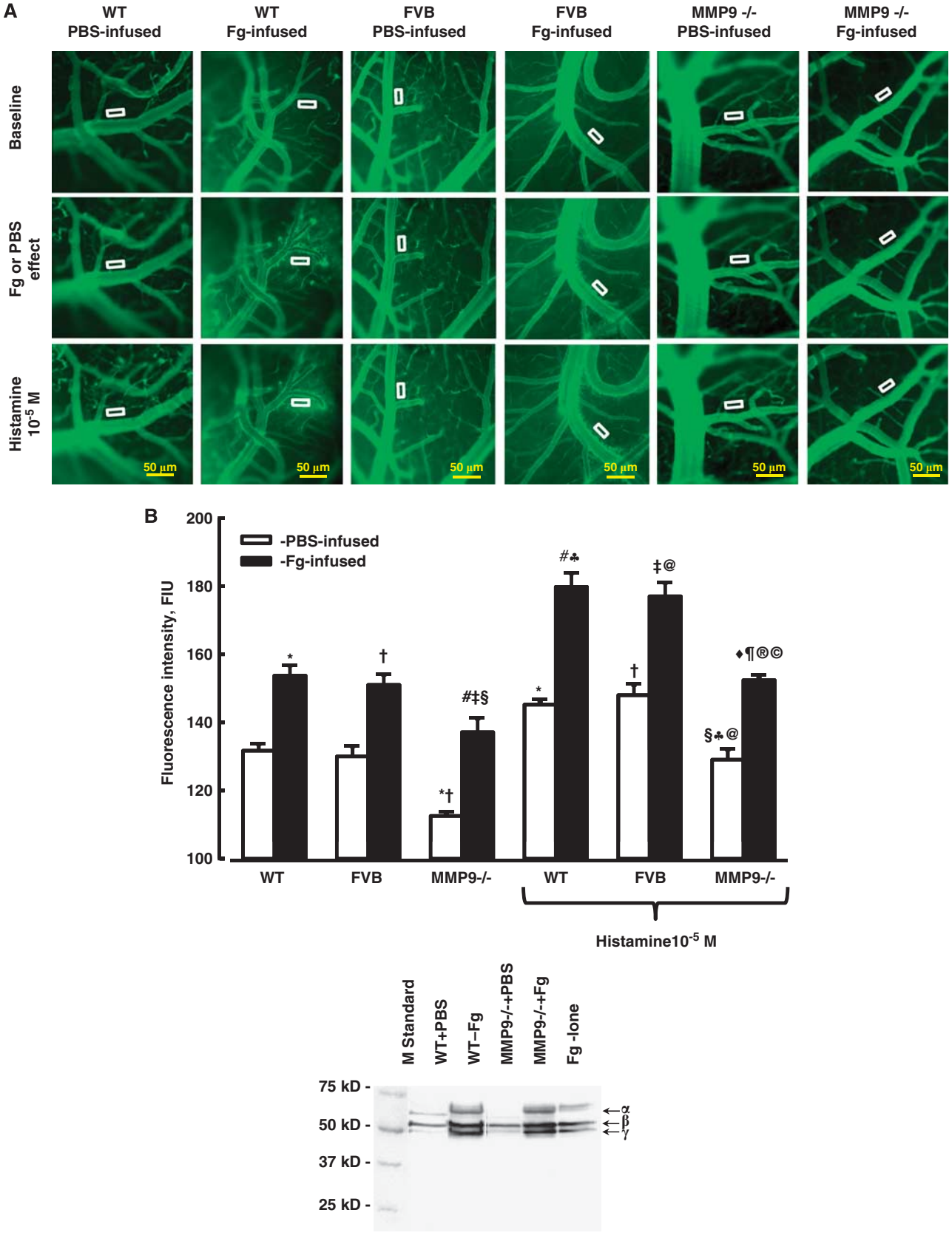

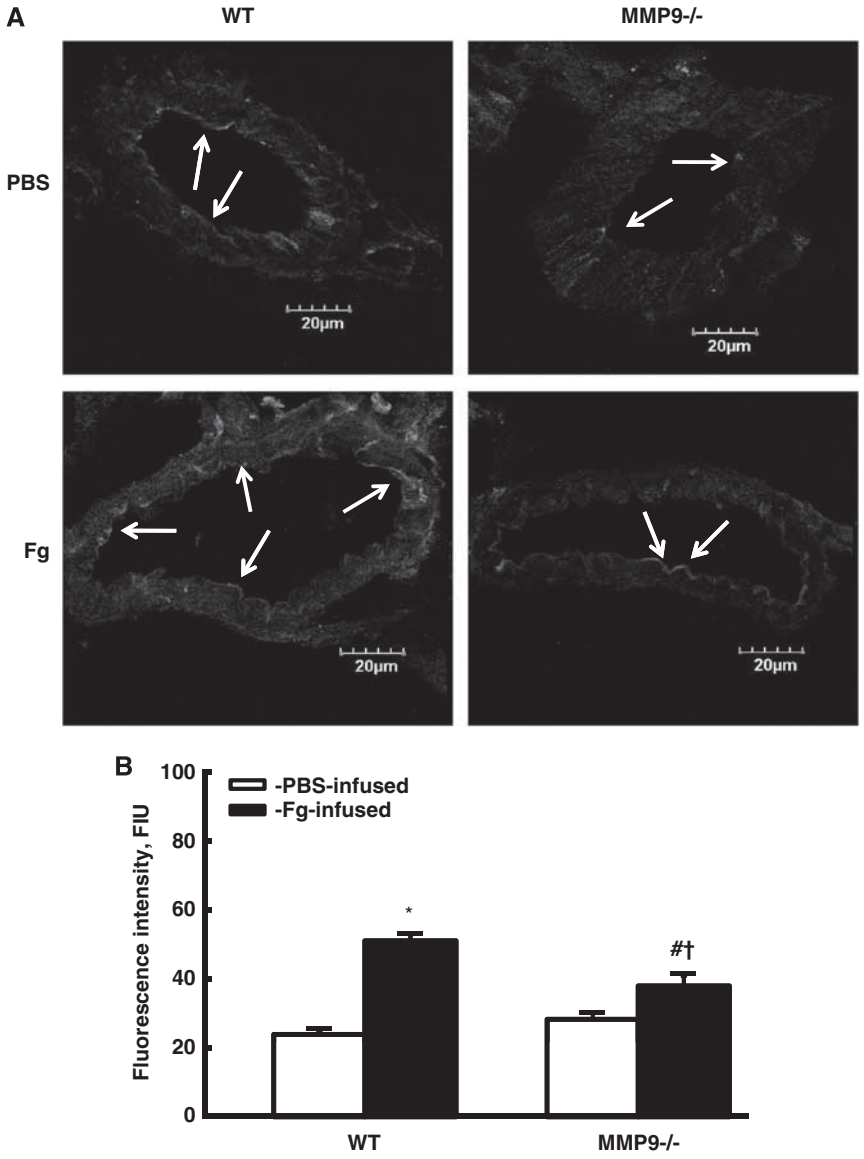

Figure 3 Expression of intercellular adhesion molecule-1 (ICAM-1) in mouse pial vessels. (**A**) Examples of vessel images in samples obtained from wild-type (WT; first column) and matrix metalloproteinase-9 (MMP-9) gene knockout (MMP9−/−; second column) mice infused with phosphate-buffered saline (PBS; first row) or fibrinogen (Fg; second row). ICAM-1 expression was assessed by the fluorescence intensity along the internal surface of a vessel. Arrows indicate expression of ICAM-1 on the internal (endothelial) surface of a vessel. (**B**) Summary of fluorescence intensity changes in vascular segments after infusion of Fg or PBS. $P < 0.05$ for all. *—versus WT + PBS, #—versus WT + Fg, †—versus (MMP9−/−) + PBS; $n = 4$ for all groups. The color reproduction of this figure is available on the *Journal of Cerebral Blood Flow and Metabolism* journal online.

No difference in Fg degradation was found in mice infused with Fg compared with that in mice infused with PBS (Figure 2, inset). These data indicate that changes in pial venular permeability occur due to alteration in blood concentration of undegraded Fg.

Infusion of Dextran-410 did not have an effect on FITC-BSA leakage from pial venules: fluorescence intensity in interstitium adjacent to a venule (119% ± 3% of baseline) was not different from that after infusion of PBS (Figure 2; 127% ± 5% of baseline). In animals infused with only FITC-BSA, its leakage from pial venules to interstitium during 1 hour was about 107% ± 1% of baseline.

ICAM-1 Expression

Endothelial expression of ICAM-1 in the brain vessels was greater after Fg (50 ± 3 FIU) than after PBS (22 ± 2 FIU) infusion in WT mice (shown with arrows in Figure 3). In MMP9−/− mice, Fg induced greater expression (39 ± 5 FIU) of endothelial ICAM-1 than infusion of PBS (24 ± 2 FIU) (Figure 3). However, expression of ICAM-1 in MMP9−/− mice was less than in WT mice after infusion of Fg, while there was no difference in ICAM-1 expression between the WT and MMP9−/− mice infused with PBS (Figure 3). In another series of experiments, there was no

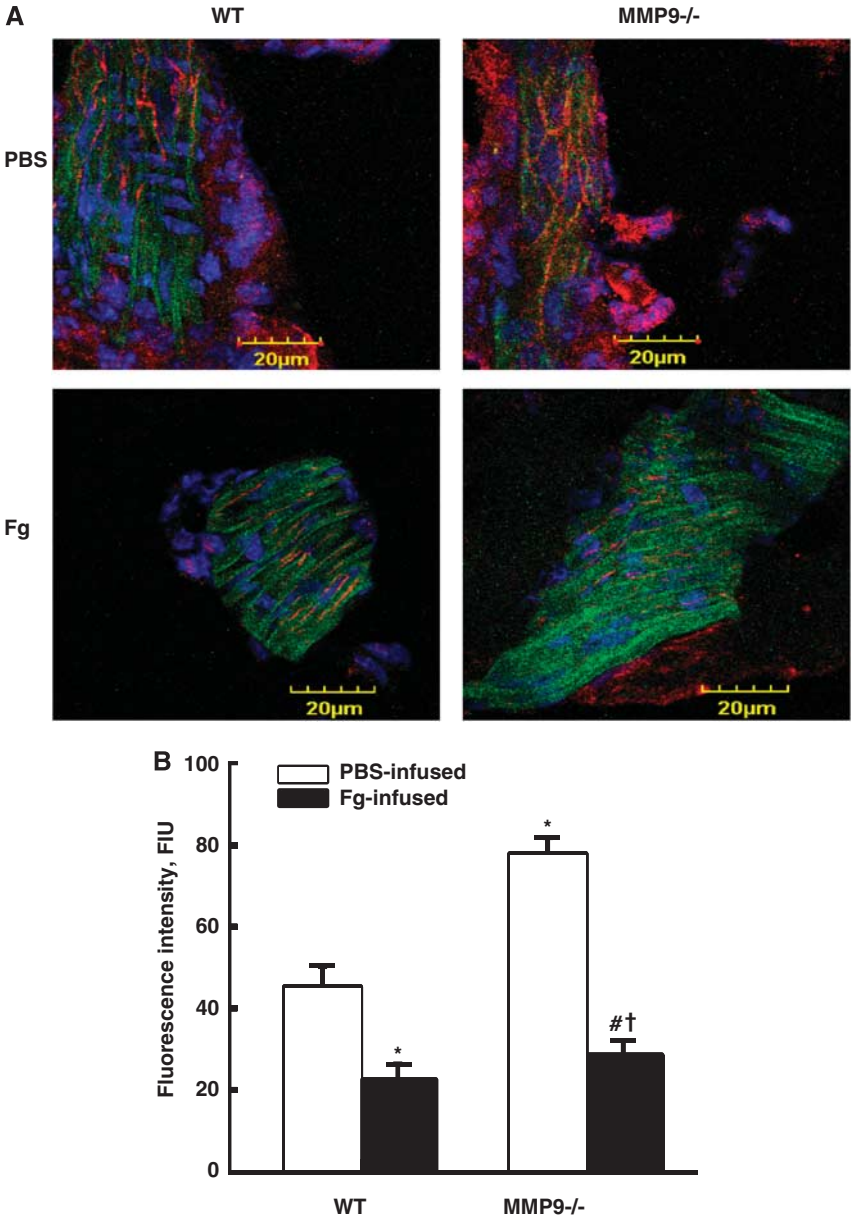

Figure 4 Expression of vascular endothelial cadherin (VE-cadherin) in mouse pial vessels. (**A**) Examples of vessel images in samples obtained from wild-type (WT; first column) and matrix metalloproteinase-9 (MMP-9) gene knockout (MMP9−/−; second column) mice infused with phosphate-buffered saline (PBS; first row) or fibrinogen (Fg; second row). VE-cadherin expression was assessed by fluorescence intensity along the vascular segment. Expression of VE-cadherin (red) in pial vessels shown with fluorescein isothiocyanate (FITC)-*Lycopersicon esculentum* agglutinin (LEA)-labeled endothelium (green) and 4,6-diamidino-2-phenyl-indole (DAPI)-labeled nuclei (blue). (**B**) Summary of fluorescence intensity changes in vascular segments after infusion of Fg or PBS. $P < 0.05$ for all. *—versus WT + PBS, #—versus WT + Fg, †—versus (MMP9−/−) + PBS; $n = 5$ for all groups.

difference in expression of ICAM between Dextran- (86.16 ± 11 FIU) and Fg-infused (73 ± 8 FIU) WT mice.

VE-Cadherin Expression

Expression of VE-cadherin in the brain cortical vessels was less after Fg (22 ± 4 FIU) than after PBS (43 ± 7 FIU) infusion in WT mice (Figure 4). In MMP9−/− mice, Fg induced lower expression (28 ± 2 FIU) of VE-cadherin than PBS (78 ± 5 FIU), although it was still greater than in WT mice (Figure 4). Expression of VE-cadherin in MMP9−/− mice was greater than in WT mice after PBS (Figure 4).

Matrix Metalloproteinase Activity by in Tissue Zymography

Fibrinogen-induced activation of MMP-9 was shown by in tissue zymography, which detects all MMPs but mainly activation of MMP-9 and MMP-2 (Mook *et al*, 2003). High blood content of Fg

increased the activity of MMPs in both WT and MMP9−/− mice (Figure 5). However, the activity of MMPs was greater after Fg infusion in WT (Figure 5; 71 ± 3 FIU) than in MMP9−/− (Figure 5; 46 ± 2 FIU) mice. Difference between activities of MMPs in Fg-infused WT and MMP9−/− mice (25 ± 1 FIU) is solely determined by activation of MMP-9. There was no difference in the activities of MMPs between PBS-infused WT and MMP9−/− mice (Figure 5). No activity of MMPs was found in groups treated with 1,10-phenanthroline (Figure 5, inset).

PV-1 Expression

The presence of LEA clearly indicated well-perfused brain vasculature. PV-1 expression in the brain cortical vessels was found in response to infusion of Fg and PBS (Figure 6). However, PV-1 expression was greater after Fg than after PBS infusion in both WT and MMP9−/− mice (Figure 6). In MMP9−/− mice, expression of PV-1 induced by Fg was less than that in WT mice (Figure 6). Similarly, expression of PV-1 after infusion of PBS was less in MMP9−/− than in WT mice (Figure 6).

Discussion

Changes in EC layer integrity, the first level of BBB, defines the permeability of cerebral vasculature (Abbott, 2000). In the present study, an effect of increased blood content of Fg on mice cerebrovascular permeability was tested *in vivo*. An elevation of blood Fg concentration resulted in a significant pial venular leakage in WT mice, suggesting that at high blood levels, Fg induces disruption of EC layer integrity leading to an enhanced macromolecular leakage. An insignificant effect on cerebrovascular leakage caused by infusion of the same volume of PBS indicates that a possible increase in hydrostatic pressure (although a very limited, particularly in venules) is less effective in causing the macromolecular leakage than that induced by Fg infusion. No FITC-BSA leakage was found in animals not treated with PBS, Fg, or Dextran, indicating that binding of Fg to its receptors on apical side of ECs causes changes in vascular wall integrity. In MMP9−/− mice, although it still induced greater pial venular leakage than PBS, an increased blood content of Fg did not have the same dramatic effect on the brain microvessels as it had in WT mice, suggesting that at high blood levels, Fg binding to EC activates MMP-9. We showed that an increase in Fg concentration increases EC layer permeability not only to albumin but to Fg itself (Tyagi *et al*, 2008). Deposited in SEM and immobilized Fg is more prone to digestion, leading to an increased production of Fg digestion products and thus exacerbating vascular remodeling and permeability (Lominadze *et al*, 2006, 2010). We did not find an increase in Fg degradation in plasma obtained from experimental animals (Figure 2, inset), suggesting that an increase in pial venular permeability was induced mainly by undegraded Fg.

Histamine released from nerve terminals, transiently 'opens' BBB (Abbott, 2000). It has been shown that histamine increases vascular permeability via contraction of ECs (Majno *et al*, 1967) and increases formation of pinocytotic vesicles in ECs (Gross *et al*, 1982). Thus, histamine affects both transcellular and paracellular pathways, and as such was an appropriate tool in the study. Our data show that histamine induced greater cerebrovascular permeability in the presence of high blood content of Fg, indicating that an increase in Fg level exacerbates cerebrovascular permeability induced by an additional insult, that is, histamine. However, the absence of MMP-9 activity still had a protective effect on histamine-induced cerebrovascular permeability mediated through both transcellular and paracellular transport pathways.

Increased blood concentration of Fg results in an increase of blood viscosity (Lominadze *et al*, 1998) and therefore an increase in blood flow shear stress (Chien *et al*, 1966). This contributes to an activation of ECs expressing and/or activating various integrins and adhesion molecules including ICAM-1 (Springer, 1990), a well-known Fg receptor (Plow *et al*, 2000). In the present study, an increase in blood Fg concentration enhanced expression of ICAM-1 in mouse brain vasculature. In MMP9−/− mice, although Fg still caused more ICAM-1 expression than PBS, it caused lesser expression of ICAM-1 than in WT mice. Earlier, we showed that Fg dose dependently binds to ICAM-1 in isolated cremaster muscle arteriol (Lominadze *et al*, 2005). Others have shown that Fg regulates activation of ICAM-1 expression in cultured human saphenous vein ECs (Harley *et al*, 2000). We now present, for the first time, an effect of increased blood content of Fg on expression of ICAM-1 in cerebral microvessels of WT and MMP-9 mice. Infusion of Dextran also increased

Figure 5 Activation of matrix metalloproteinases (MMPs) in mouse pial vessels. (**A**) Examples of vessel images in samples obtained from wild-type (WT; first column) and MMP-9 gene knockout (MMP9−/−; second column) mice infused with phosphate-buffered saline (PBS; first row) or fibrinogen (Fg; second row). MMP activity was assessed by fluorescence intensity (green) along the pial vascular segment. 4,6-Diamidino-2-phenyl-indole (DAPI)-labeled cellular nuclei are shown in blue. (**B**) Summary of fluorescence intensity changes in the brain vessels after infusion of Fg or PBS. $P < 0.05$ for all. *—versus WT + PBS, #—versus WT + Fg, †—versus (MMP9−/−) + PBS; $n = 4$ for all groups. Inset: Validity of the test was confirmed in parallel series of experiments done on WT and MMP9−/− mice. The brain cryopreserved slices were treated with 1,10-phenanthroline,monohydrate a general metalloproteinase inhibitor (green) as a negative control. Cell nuclei are labeled with DAPI (blue). The color reproduction of this figure is available on the *Journal of Cerebral Blood Flow and Metabolism* journal online.

expression of ICAM-1 in mouse brain vessels, suggesting that increase in blood viscosity and thus in shear stress by an increase in blood content of Fg or Dextran may enhance expression of ICAM-1. However, Dextran did not cause an increase in pial venular permeability to albumin, suggesting that just an overexpression of

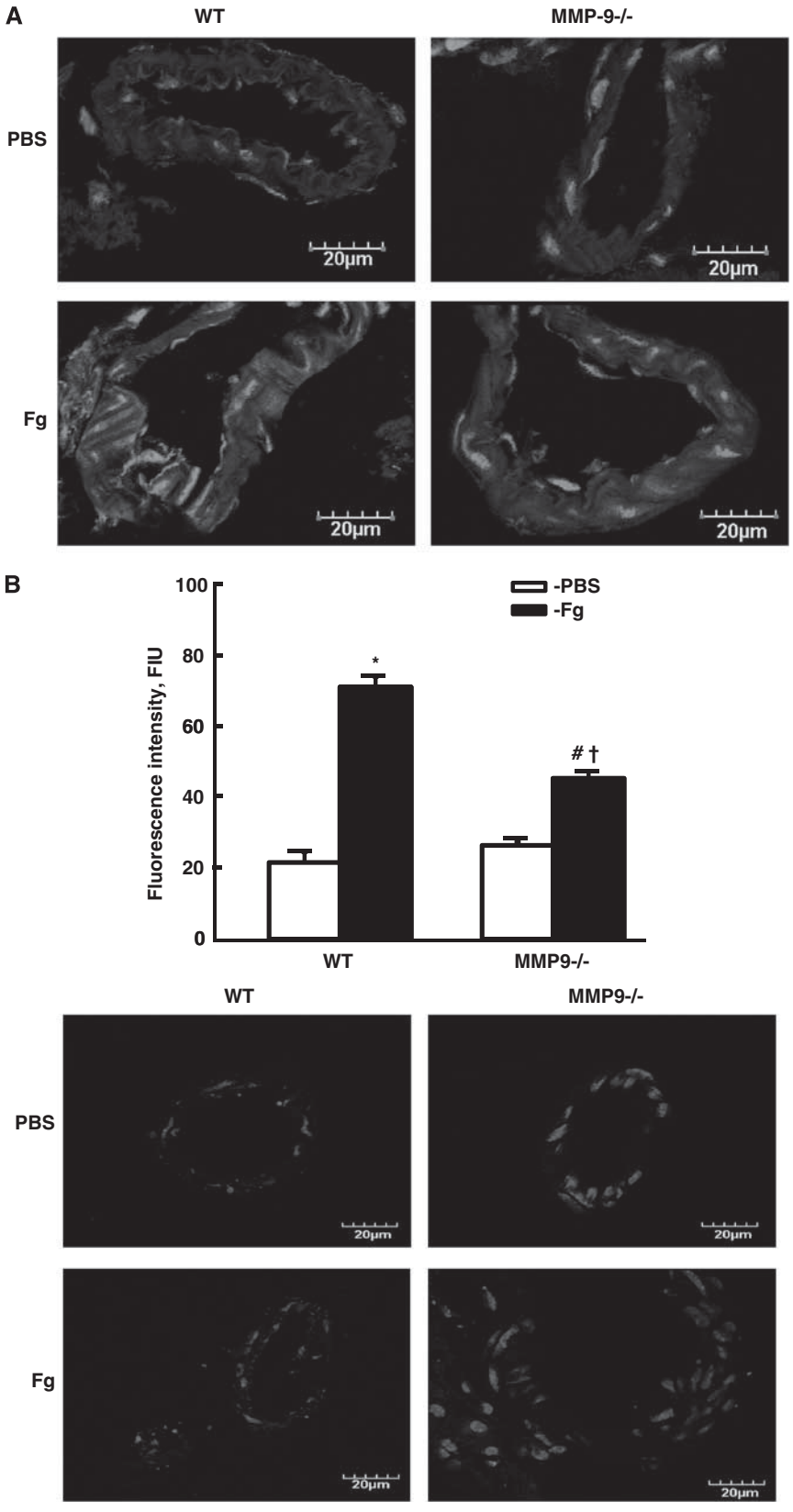

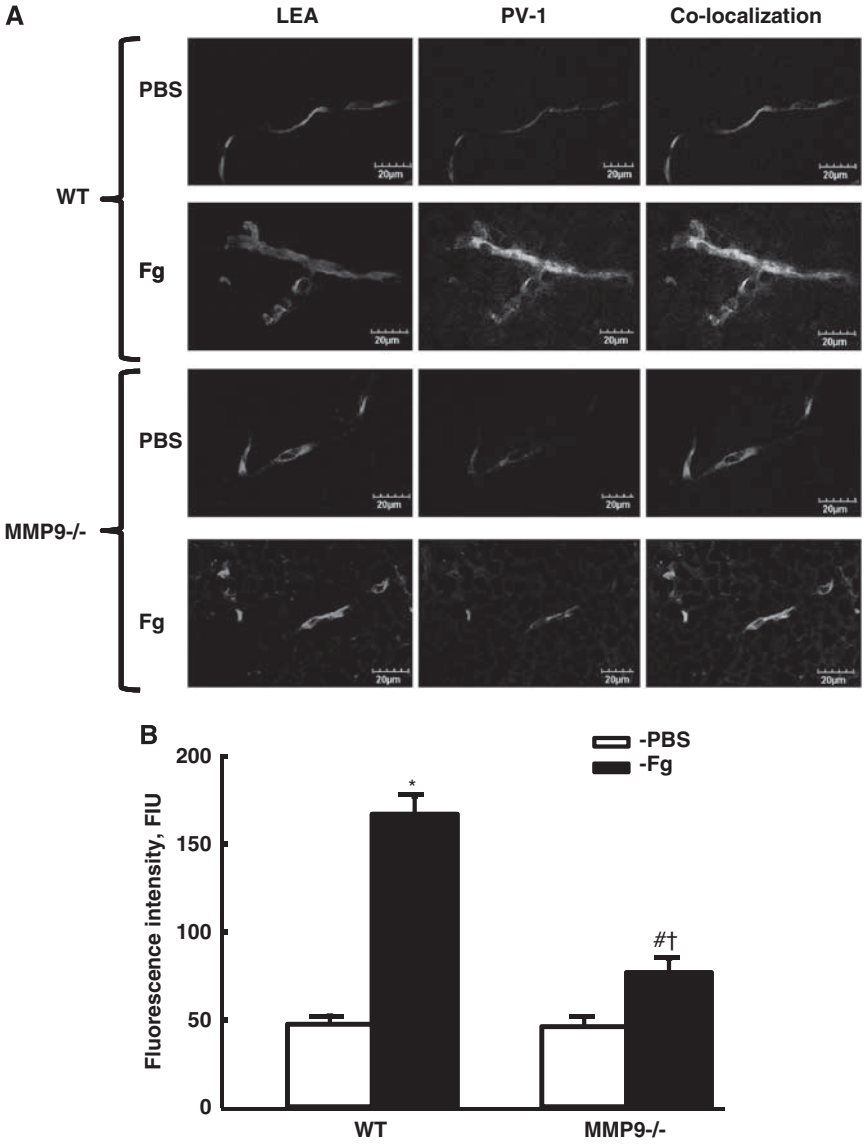

Figure 6 Expression of plasmalemmal vesicle-associated protein-1 (PV-1) in mouse pial vessels. (**A**) Examples of vessel images in samples obtained from wild-type (WT; two upper rows) and matrix metalloproteinase-9 (MMP-9) gene knockout (MMP9−/−; two bottom rows) mice infused with phosphate-buffered saline (PBS) or fibrinogen (Fg). First column represents tetramethylrhodamine β-isothiocyanate-*Lycopersicon esculentum* agglutinin (TRITC-LEA)-labeled blood vessels (red). PV-1 expression (green) in the same vessel is shown in the second column. The third column represents images with colocalization of LEA and PV-1 in the observed vessels. PV-1 expression was assessed by fluorescence intensity along the vascular segment. (**B**) Summary of fluorescence intensity changes in vascular segments after infusion of Fg or PBS. $P < 0.05$ for all. *—versus WT + PBS, #—versus WT + Fg, †—versus (MMP9−/−) + PBS; $n = 5$ for all groups. The color reproduction of this figure is available on the *Journal of Cerebral Blood Flow and Metabolism* journal online.

ICAM-1 may not be enough to trigger the vascular wall disruption and cause an increase in vascular permeability. An enhanced binding of Fg to endothelial ICAM-1 and activation of this endothelial molecule may be necessary to increase vascular permeability to proteins. The presence of ICAM-1 on VSMCs (vascular smooth muscle cells) is also shown in Figure 3. Since we have shown that at pathologically high levels, Fg penetrates EC layer (Tyagi *et al*, 2008) and may also bind to ICAM-1 on VSMCs (Lominadze *et al*, 2005), role of Fg binding to ICAM-1 on VSMCs needs further investigation.

Binding of Fg to ICAM-1 activates ERK-1/2 signaling pathway in ECs (Sen *et al*, 2009), which is known to trigger activation of MMPs through formation of reactive oxygen species (Touyz, 2006). Therefore, an increased binding of Fg to endothelial ICAM-1 can cause MMP-9 activation, possibly through formation of reactive oxygen species. Traumatic brain injury-induced inflammation has been associated with

increased expression of ICAM-1 and MMP-9 (Knoblach and Faden, 2004). The present data indicate that increased content of Fg leads to activation of MMPs and particularly MMP-9, suggesting a possibility that an activated MMP-9 may further exacerbate destruction of the EC layer.

Previously, we showed that increased content of Fg affects endothelial junction proteins and induces formation of F-actin (filamentous actin) (Tyagi *et al*, 2008). Since actin is connected to the most junction proteins (including VE-cadherin), formation of F-actin may be a mechanism for translocation of occludin, zona occludin-1, and zona occludin-2 seen previously (Patibandla *et al*, 2009). These changes may increase gaps between ECs and enhance vascular permeability (Lominadze *et al*, 2010). Increased macromolecular leakage of pial venules in the present study could directly be associated with Fg-induced downregulation of endothelial tight junction proteins and the resultant EC gap formation found in earlier studies (Patibandla *et al*, 2009; Tyagi *et al*, 2008). In addition to tight junction proteins and tight junction-associated proteins, higher levels of Fg cause downregulation of the adherence junction protein VE-cadherin in mouse cerebral vessels. These results coincide with our previous data, indicating that increased content of Fg downregulates VE-cadherin expression in cultured mouse brain endothelial cells (Muradashvili *et al*, 2011). Combined, these data indicate that increased content of Fg may enhance vascular permeability altering a paracellular transport pathway. The lesser effect of Fg on VE-cadherin expression in vessels of MMP9−/− mice suggests that Fg-induced activation of MMP-9 may have a role in expression of VE-cadherin. Functional effects of MMP-9 on expression of VE-cadherin and Fg-induced changes in cell junctional interactions in mouse brain endothelial cells were recently demonstrated (Muradashvili *et al*, 2011). In addition, it has been shown that activated MMP-9 degrades VE-cadherin (Navaratna *et al*, 2007). Thus, Fg-induced activation of MMP-9 can cause degradation of VE-cadherin, leading to an increased cerebrovascular permeability.

In the absence of MMP-9 activity, an increased blood content of Fg caused greater pial venular leakage than infusion of PBS, indicating that in addition to paracellular transport, another transport mechanism may also be involved. The length of a typical trinodular structure of Fg is about 46 nm (Marchant *et al*, 2002), while its Stokes radius is about 8.4 nm (Potschka, 1987), which is significantly greater than that of albumin (3.6 nm; Michel and Curry, 1999). Therefore, both Fg and albumin can easily be taken up by caveolae, which can be about 70 to 80 nm in diameter (Simionescu *et al*, 2009), migrated through, and be released at the basal side of the cell. All these points to a possibility that at increased blood content of Fg, macromolecules such as albumin and Fg itself can be taken up by caveolae.

Upregulation of PV-1 in the brain vasculature during BBB disruption in rodents has already been demonstrated (Shue *et al*, 2008). Our finding that increased blood content of Fg causes greater formation of PV-1 in WT than in MMP9−/− mice indicates that at high level, Fg may enhance a transendothelial transport through activation of MMP-9. A possible role of MMP-9 activity in Fg-induced PV-1 formation suggests that activation of MMP-9 directly correlates with formation of PV-1, that is, caveolae and fenestrae. A possible involvement of transendothelial transport mechanism in Fg-mediated microvascular leakage is suggested by the finding that at high blood content of Fg cerebrovascular permeability was associated with increased expression of PV-1 in mouse brain vessels. The prevailing role of Fg-induced transendothelial versus paracellular mechanism has yet to be determined.

In conclusion, the present study shows that at an increased blood level, Fg causes macromolecular leakage of pial venules in mice, which may involve both transcellular and paracellular pathways. There is evidence that both these pathways can be governed by activation of MMP-9. Thus, the present study suggests a possible role of increased Fg content in alteration of BBB, leading to edema, which can be a complicating factor during inflammatory cerebrovascular pathologies, such as stroke and traumatic brain injury.

Limitations of the Study

Since we measured only the relative fluorescence intensity in the interstitial space adjacent to a pial venule and did not evaluate hydrostatic pressure in the venule, we could not assess the venular permeability to solutes as required by the Starling's concept. However, the presented data indicate an accumulation of FITC-BSA in interstitium, which can be considered an adequate measure for a venular permeability to proteins. In addition, we have measured vascular diameters and systemic blood pressures, which were not changed in response to Fg or PBS infusion in all groups of mice. We also measured fluorescence intensity in target venules and found it to be decreased after infusion of Fg. This can be explained by decreased arteriolar diameters in response to an increased blood content of Fg (Lominadze *et al*, 2005, 2010) and leakage of FITC-BSA from a vessel to interstitium. Combined with the fluorescence intensity increase in interstitium, these data suggest even a greater effect of Fg in disruption of BBB.

Disclosure/conflict of interest

The authors declare no conflict of interest.

References

Abbott NJ (2000) Inflammatory mediators and modulation of blood-brain barrier permeability. *Cell Mol Neurobiol* 20:131–47

Chien S, Usami S, Taylor HM, Lundberg JL, Gregersen MI (1966) Effects of hematocrit and plasma proteins on human blood rheology at low shear rates. *J Appl Physiol* 21:81–7

Cohen ZVI, Bonvento G, Lacombe P, Hamel E (1996) Serotonin in the regulation of brain microcirculation. *Prog Neurobiol* 50:335–62

Danesh J, Lewington S, Thompson SG, Lowe GD, Collins R, Kostis JB, Wilson AC, Folsom AR, Wu K, Benderly M, Goldbourt U, Willeit J, Kiechl S, Yarnell JW, Sweetnam PM, Elwood PC, Cushman M, Psaty BM, Tracy RP, Tybjaerg-Hansen A, Haverkate F, de Maat MP, Fowkes FG, Lee AJ, Smith FB, Salomaa V, Harald K, Rasi R, Vahtera E, Jousilahti P, Pekkanen J, D'Agostino R, Kannel WB, Wilson PW, Tofler G, Arocha-Pinango CL, Rodriguez-Larralde A, Nagy E, Mijares M, Espinosa R, Rodriquez-Roa E, Ryder E, Diez-Ewald MP, Campos G, Fernandez V, Torres E, Coll E, Marchioli R, Valagussa F, Rosengren A, Wilhelmsen L, Lappas G, Eriksson H, Cremer P, Nagel D, Curb JD, Rodriguez B, Yano K, Salonen JT, Nyyssonen K, Tuomainen TP, Hedblad B, Lind P, Loewel H, Koenig W, Meade TW, Cooper JA, De Stavola B, Knottenbelt C, Miller GJ, Bauer KA, Rosenberg RD, Sato S, Kitamura A, Naito Y, Iso H, Rasi V, Palosuo T, Ducimetiere P, Amouyel P, Arveiler D, Evans AE, Ferrieres J, Juhan-Vague I, Bingham A, Schulte H, Assmann G, Cantin B, Lamarche B, Despres JP, Dagenais GR, Tunstall-Pedoe H, Woodward M, Ben Shlomo Y, Davey SG, Palmieri V, Yeh JL, Rudnicka A, Ridker P, Rodeghiero F, Tosetto A, Shepherd J, Ford I, Robertson M, Brunner E, Shipley M, Feskens EJ, Kromhout D, Fibrinogen SC (2005) Plasma fibrinogen level and the risk of major cardiovascular diseases and nonvascular mortality: an individual participant meta-analysis. *JAMA* 294:1799–809

del Zoppo GJ, Levy DE, Wasiewski WW, Pancioli AM, Demchuk AM, Trammel J, Demaerschalk BM, Kaste M, Albers GW, Ringelstein EB (2009) Hyperfibrinogenemia and functional outcome from acute ischemic stroke. *Stroke* 40:1687–91

Eidelman RS, Hennekens CH (2003) Fibrinogen: a predictor of stroke and marker of atherosclerosis. *Eur Heart J* 24:499–500

Gaffney PJ (2001) Fibrin degradation products: a review of structures found *in vitro* and *in vivo*. *Ann NY Acad Sci* 936:594–610

Gross PM, Teasdale GM, Graham DI, Angerson WJ, Harper AM (1982) Intra-arterial histamine increases blood-brain transport in rats. *Am J Physiol Heart Circ Physiol* 243:H307–17

Harley SL, Sturge J, Powell JT (2000) Regulation by fibrinogen and its products of intercellular adhesion molecule-1 expression in human saphenous vein endothelial cells. *Arterioscler Thromb Vasc Biol* 20: 652–8

Hicks RCJ, Golledge J, Mir-Hasseine R, Powell JT (1996) Vasoactive effects of fibrinogen on saphenous vein. *Nature* 379:818–20

Hnasko R, McFarland M, Ben-Jonathan N (2002) Distribution and characterization of plasmalemma vesicle protein-1 in rat endocrine glands. *J Endocrinol* 175:649–61

Johnson A, Garcia-Szabo R, Kaplan JE, Malik AB (1985) Fibrin degradation products increase lung transvascular fluid filtration after thrombin-induced pulmonary microembolism. *Thromb Res* 37:543–54

Knoblach SM, Faden AI (2004) Administration of either anti-intercellular adhesion molecule-1 or a nonspecific control antibody improves recovery after traumatic brain injury in the rat. *J Neurotrauma* 19:1039–50

Landin K, Tengborn L, Smith U (1990) Elevated fibrinogen and plasminogen activator inhibitor (PAI-1) in hypertension are related to metabolic risk factors for cardiovascular disease. *J Intern Med* 227:273–8

Lominadze D, Dean WL, Tyagi SC, Roberts AM (2010) Mechanisms of fibrinogen-induced microvascular dysfunction during cardiovascular disease. *Acta Physiol* 198:1–13

Lominadze D, Joshua IG, Schuschke DA (1998) Increased erythrocyte aggregation in spontaneously hypertensive rats. *Am J Hypertens* 11:784–9

Lominadze D, Roberts AM, Tyagi N, Tyagi SC (2006) Homocysteine causes cerebrovascular leakage in mice. *Am J Physiol Heart Circ Physiol* 290:H1206–13

Lominadze D, Tsakadze N, Sen U, Falcone JC, D'Souza SE (2005) Fibrinogen- and fragment D-induced vascular constriction. *Am J Physiol* 288:H1257–64

Majno G, Gilmore V, Leventhal M (1967) On the mechanism of vascular leakage caused by histamine-type mediators: a microscopic study *in vivo*. *Circ Res* 21:833–48

Manwaring D, Curreri PW (1981) Cellular mediation of respiratory distress syndrome induced by fragment D. *Ann Chir Gynaecol* 70:304–7

Marchant RE, Kang I, Sit PS, Zhou Y, Todd BA, Eppell SJ, Lee I (2002) Molecular views and measurements of hemostatic processes using atomic force microscopy. *Curr Protein Pept Sci* 3:249–74

Mehta D, Malik AB (2006) Signaling mechanisms regulating endothelial permeability. *Physiol Rev* 86:279–367

Michel CC, Curry FE (1999) Microvascular permeability. *Physiol Rev* 79:703–61

Mook ORF, Overbeek CV, Ackema EG, Maldegem FV, Frederiks WM (2003) *In situ* localization of gelatinolytic activity in the extracellular matrix of metastases of colon cancer in rat liver using quenched fuorogenic DQ-gelatin. *J Histochem Cytochem* 51:821–9

Mozer A, Whittemore S, Benton R (2010) Spinal microvascular expression of PV-1 is associated with inflammation, perivascular astrocyte loss, and diminished EC glucose transport potential in acute SCI. *Curr Neurovasc Res* 7:238–50

Muradashvili N, Tyagi N, Tyagi R, Munjal C, Lominadze D (2011) Fibrinogen alters mouse brain endothelial cell layer integrity affecting vascular endothelial cadherin. *Biochem Biophys Res Commun* 413:509–14

Nakamura A, Kohsaka T, Johns EJ (1996) Neuro-regulation of interleukin-6 gene expression in the spontaneously hypertensive rat kidney. *J Hypertension* 14:839–45

Navaratna D, McGuire PG, Menicucci G, Das A (2007) Proteolytic degradation of VE-cadherin alters the blood-retinal barrier in diabetes. *Diabetes* 56:2380–7

Patibandla PK, Tyagi N, Dean WL, Tyagi SC, Roberts AM, Lominadze D (2009) Fibrinogen induces alterations of endothelial cell tight junction proteins. *J Cell Physiol* 221:195–203

Plow EF, Haas TA, Zhang L, Loftus J, Smith JW (2000) Ligand binding to integrins. *J Biol Chem* 275:21785–8

Potschka M (1987) Universal calibration of gel permeation chromatography and determination of molecular shape in solution. *Anal Biochem* 162:47–64

Rosell A, Ortega-Aznar A, Alvarez-Sabin J, Fernandez-Cadenas I, M, Molina CA, Lo EH, Montaner J (2006) Increased brain expression of matrix metalloproteinase-9 after ischemic and hemorrhagic human stroke. *Stroke* 37:1399–406

Rosenblum WI, El-Sabban F (1982) Influence of shear rate on platelet aggregation in cerebral microvessels. *Microvasc Res* 23:311–5

Sen U, Tyagi N, Patibandla PK, Dean WL, Tyagi SC, Roberts AM, Lominadze D (2009) Fibrinogen-induced endothelin-1 production from endothelial cells. *AJP Cell Physiol* 296:C840–7

Shue E, Carson-Walter E, Liu Y, Winans B, Ali Z, Chen J, Walter K (2008) Plasmalemmal vesicle associated protein-1 (PV-1) is a marker of blood-brain barrier disruption in rodent models. *BMC Neurosci* 9:29

Simionescu M, Popov D, Sima A (2009) Endothelial transcytosis in health and disease. *Cell Tissue Res* 335:27–40

Springer TA (1990) Adhesion receptors of the immune system. *Nature* 346:425–34

Touyz RM (2006) Mitochondrial redox control of matrix metalloproteinase signaling in resistance arteries. *Arterioscler Thromb Vasc Biol* 26: 685–8

Tyagi N, Roberts AM, Dean WL, Tyagi SC, Lominadze D (2008) Fibrinogen induces endothelial cell permeability. *Mol Cell Biochem* 307:13–22

Vestweber D (2008) VE-Cadherin: the major endothelial adhesion molecule controlling cellular junctions and blood vessel formation. *Arterioscler Thromb Vasc Biol* 28:223–32